

A COMPREHENSIVE KINETICS MODEL FOR CO OXIDATION DURING CHAR COMBUSTION

Greg Haussmann and Charles Kruger

Department of Mechanical Engineering
Stanford University, Stanford, CA 94305

INTRODUCTION:

The most important parameter in representing energy feedback to a particle during char combustion concerns the oxidation of CO to CO₂. If substantial oxidation of CO occurs near a particle, then the greater heat of combustion for the complete oxidation of carbon to CO₂ (94.1 kcal/mole vs. 26.4 kcal/mole for oxidation to CO) is available for energy feedback mechanisms. "Energy feedback" is here defined as any situation in which an individual particle receives a significant fraction of its heat of combustion directly, through the localized oxidation of emitted combustible species, i.e. CO. Conversely, if the oxidation of CO does not occur near a particle, then energy feedback will only occur indirectly, through heating of the bulk gas. The primary reaction product at the particle surface during char combustion is generally considered to be CO, and the location of the subsequent CO oxidation zone plays a very important role in determining the particle temperature. Ayling and Smith (1) performed experimental and modeling work which indicates that CO oxidation is not of major importance under the conditions they investigated, although they noted a need for improved accuracy in measuring char reactivities, as well as for better modeling of the gas phase CO oxidation kinetics. The modeling work presented in this paper attempts to develop an improved understanding of the boundary layer oxidation of CO through the use of a comprehensive set of kinetics expressions. It is hoped that the use of a fundamental set of kinetics expressions will more accurately represent the transient conditions occurring around an oxidizing char particle, when compared to the use of global kinetics expressions. The transport and energy equations are solved, generating both species and temperature profiles surrounding a single particle.

MODEL DEVELOPMENT:

The CO oxidation model developed at Stanford currently employs a number of assumptions, which are listed in Table 1. One critical assumption used is the restriction that the only mass fluxes at the particle surface are CO and O₂. The species mass transport equation used assume convective and diffusive transport only, with source terms calculated from the kinetics expressions. The gas phase reactions are modeled through the use of a subset of a set of expressions developed by Westbrook, et al (2) to study the pyrolysis and oxidation of ethylene. This subset is listed in Table 2. The success of this model in predicting the properties of a laminar ethylene flame suggests that it is also valid for the more simple fuels contained as subsets (i.e. CO).

The basic equation for mass transport in the particle boundary layer is below.

$$\underbrace{\frac{d}{dr} \left[\frac{\rho_1}{\rho} \dot{m}_c 4\pi r^2 \right]}_{\text{Convection}} - \underbrace{\frac{d}{dr} \left[4\pi r^2 \rho D_1 \frac{d}{dr} (\rho_1/\rho) \right]}_{\text{Diffusion}} = \underbrace{4\pi r^2 \dot{p}_1}_{\text{Source}} \quad (1)$$

where

- ρ_1 = Mass fraction of species 1
- ρ = Density of local gas mixture, gm/cm³
- \dot{m}_c'' = Carbon flux at particle surface, gm/cm²/sec
- a = Particle radius, cm
- D_1 = Diffusion coefficient for species 1, cm²/sec
- \dot{p}_1 = Source term for species 1 (from kinetics), gm/cm³/sec

Equation 1 is non-dimensionalized through the use of the parameters below.

- $y = \frac{a/r}{(\rho_1/\rho)}$ Non-dimensional coordinate
- $X_1 = \frac{(\rho_1/\rho)}{(\rho_1/\rho)_\infty}$ Non-dimensional mass fraction
- $\beta_1 = (\rho_1/\rho)_\infty \rho D_1 / (a \dot{m}_c'')$ Non-dimensional diffusion coefficient
- $S_1 = a \dot{p}_1 / (y^4 \dot{m}_c'')$ Non-dimensional source term

The resulting form for the transport equation is:

$$F_1 = (\rho_1/\rho)_\infty X_1 + \beta_1 \frac{dX_1}{dy} \quad 2a)$$

$$\frac{dF_1}{dy} = -S_1 \quad 2b)$$

In equation 2a, the term F_1 represents a non-dimensional flux, for species 1. The two equations above are solved, with the boundary conditions being:

$$\begin{aligned} X_1(y=1) &= 1 \\ F_1(y=1) &= 0 \quad \text{except for:} \quad \begin{aligned} F_{CO}(y=1) &= 28/12 \\ F_{O_2}(y=1) &= -16/12 \end{aligned} \end{aligned}$$

For $i = CO, CO_2, O_2, Ar, H_2O, O, H, OH, H_2$

The mass transport equations in the boundary layer are solved along with a simple form of the energy equation, which is similar to the transport equation used.

$$K_g \frac{d}{dr} r^2 \frac{dT}{dr} - C_g \dot{m}_c'' a^2 \frac{dT}{dr} = r^2 \dot{q}''' \quad 3)$$

where Conduction Convection Source

K_g = The average bulk thermal conductivity, erg/cm sec K

C_g = The average bulk heat capacity, erg/gm K

As with the species transport equation, this equation is transformed into non-dimensional coordinates.

$$\frac{d^2 T}{dy^2} + \left[\frac{C_g \dot{m}'' a}{K_g} \right] \frac{dT}{dy} - \left[\frac{a^2}{K_g y^4} \right] \dot{q}'''(y) = 0 \quad (4)$$

The solution procedure utilized to solve the mass and energy transport equations is outlined in Table 3. The solution is first broken down into two components. The first part, $x_{i,1}(y)$ represents the solution to the homogenous portion of equations 2a and 2b, i.e. with no gas phase reactions occurring ($S_i = 0$). In this case the homogeneous solution takes a particularly simple analytical form.

$$x_{i,1}(y) = \frac{F_i}{(\rho_i/\rho)_\infty} + \left[1 - \frac{F_i}{(\rho_i/\rho)_\infty} \right] \exp\left[\frac{-(\rho_i/\rho)_\infty y}{D_i} \right] \quad (5)$$

The complete solution is then represented as the sum of this homogeneous term and an inhomogeneous term, $x_i'(y)$. The boundary conditions on this inhomogeneous term now become particularly simple, being $x_i'(y=1) = 0$. One nice feature of this solution technique is that it allows the general character of the solution to be calculated immediately (the homogeneous solution), while the more difficult inhomogeneous portion can be dealt with separately. The inhomogeneous portion represents a very stiff equation, and a relaxation technique is applied to reach a solution. The species and energy equations are solved in series, as indicated in Table 3, and this procedure is repeated until a desired convergence criterion has been achieved.

MODEL RESULTS:

The input parameters required for this model, and the typical "base case" values used, are listed in Table 4. The values for the base case have been chosen to match conditions measured experimentally in the Stanford flow-tube reactor, in which the independent variation of many of the important reaction parameters is possible, in particular the bulk gas temperature, the oxygen concentration, and the particle size. For the current modeling results the input parameters have been independently varied around the single base case determined from the flow-tube reactor, without attempting to represent the interdependencies of the parameters. The base case value for the char reactivity at 1800K of 0.03 gm carbon/cm²/sec agrees very well with typical values measured for char reactivities (Smith (3)), although the free stream species concentrations in the Stanford flow-tube reactor can be significantly different than those found in typical pulverized coal combustion applications. The importance of this will be discussed later.

A typical temperature profile in the particle boundary layer is presented in Figure 1. The lower curve is the solution with no gas phase reactions, while the upper curve shows the effect of CO oxidation in the boundary layer. The case chosen is one in which the greatest effect of boundary layer CO oxidation was observed, although all cases show similar profiles. In both curves the particle temperature is substantially above the bulk gas temperature (by about 500K), with this temperature overshoot increased by about 60K when gas phase CO oxidation was included. Figure 1 indicates that one way to represent the effect of CO oxidation on the particle temperature would be to look at the increase in the particle surface temperature over that with no gas phase CO oxidation. This parameter has been calculated while parametrically varying the variables listed in Table 4, and the results are discussed below.

The dependence of the bulk gas oxygen concentration is seen in Figure 2. The dependence is a reasonably strong one, although for the conditions studied the temperature increase due to CO oxidation in the boundary layer is fairly low. Thus

the energy feedback due to CO oxidation, while not negligible, is not considered to be a dominant mechanism under these conditions. It is important to note that although the base case chosen indicates little CO oxidation in the boundary layer, the trends observed will give the relative importance of the various parameters studied.

The dependence on the bulk gas water concentration is seen in Figure 3. This parameter is important due to the limiting gas phase reaction $\text{CO} + \text{OH} \rightarrow \text{CO}_2 + \text{H}$. At low concentrations there is a strong dependence of the temperature increase due to CO oxidation in the boundary layer on the bulk gas water concentration, and this dependence tails off at higher concentrations. One reason that the temperature increase is relatively low for the base case considered in the current study is that the water concentrations present in the Stanford reactor are relatively low. The only source of water in the Stanford flow-tube reactor is the moisture and hydrogen present in the coal fed into the reactor, and the relatively low particle concentrations present (< 10 particles/cm³) results in low water concentrations. Future work will consider conditions in which the water concentrations are at higher values, since this looks like a crucial parameter in studying gas phase CO oxidation, and many pulverized coal combustion environments involve water concentrations substantially above those seen in the Stanford flow-tube reactor.

The dependence of the temperature increase on the char reactivity is seen in Figure 4. The temperature increase is a relatively strong function of the char reactivity, but eventually becomes less important. This leveling off of the curve is the result of two competing processes. As the char reactivity is increased, the amount of CO present in the particle boundary layer increases, which increases the energy release due to CO oxidation near the particle. A competing effect with this is the resulting increase of the convective term in the heat transfer equation, which tends to reduce the feedback of energy released in the boundary layer back to the particle as the char reactivity increases. The net effect of these two processes is the leveling off of the curve seen in Figure 4.

The dependence on the particle radius is seen in Figure 5. It is important to note that the char reactivity has been held constant in this parametric run, while in reality the char reactivity is a strong function of the particle radius, and this must be taken into consideration in order to better represent the true effect of the particle radius. For a fixed reactivity, however, the temperature increase due to CO oxidation is a strong function of the particle radius, a quadratic type of dependence. This is due primarily to the increased heat transfer from a smaller particle to the surroundings, which tends to lessen the effect of boundary layer CO oxidation. The actual effect of particle size is some combination of this effect with the strong increase in the particle reactivity as the radius is decreased. These two effects result in opposing trends, so the net effect of the particle radius is not clear at this point.

The dependence on the bulk gas temperature is seen in Figure 6. Again there is an interdependence between this parameter and the char reactivity, a very strong influence which is not represented in the current modeling work. As expected, the effect of CO oxidation in the boundary layer is a very strong (exponential) function of the bulk gas temperature. A temperature increase of about 60K is seen at a bulk gas temperature of 2000K. When the accompanying effect of the char reactivity dependence on the temperature is included, an even stronger dependence of the temperature increase due to CO oxidation is expected.

CONCLUSIONS:

For the conditions studied, the effect of CO oxidation in the boundary layer during char combustion does not appear to be of major importance. It is important to note that the model input parameters studied were designed to simulate conditions present in the Stanford flow-tube reactor, and that the importance of boundary layer CO oxidations in typical pulverized coal combustion environments has not yet been studied with this model.

The interdependencies between the model input parameters need to be modeled in order to better represent the actual processes occurring during CO oxidation. In particular, the parameters which indicates the possibility of a strong synergistic interaction are the water concentration, oxygen concentration, and/or the bulk gas temperature with the char reactivity.

The model results indicate the relative importance of the various parameters. The water concentration is considered to be a crucial parameter for two reasons. First, it has a strong influence on OH concentration in the particle boundary layer, which in turn plays a dominant role in the oxidation kinetics of CO. Secondly, many pulverized coal combustion environments are expected to have substantially higher water concentrations than that chosen for the base case condition used with this model. Other parameters which appear to be very important are the bulk gas temperature and the oxygen concentration, especially when their influence on the char reactivity is taken into account.

REFERENCES:

1. Ayling, A.B. and I.W. Smith, "Measured Temperatures of Burning Pulverized-Fuel Particles, and the Nature of the Primary Reaction Product", *Combustion and Flame*, V 18, 1972, pp. 173-184.
2. Westbrook, C.K., Dryer, F.L., and Schug, K.P., "A Comprehensive Mechanism for the Pyrolysis and Oxidation of Ethylene", 19th Symposium (Int'l) on Combustion, The Combustion Institute, 1982, pp. 153-166.
3. I.W. Smith, "The Combustion Rates of Coal Chars: a Review", 19th Symposium (Int'l) on Combustion, The Combustion Institute, 1982, pp. 1045-1065.

TABLE 1. ASSUMPTIONS

- Steady State.
- Diffusive and convective transport only.
- Constant particle radius.
- Spherical symmetry.
- Surface mass flux is given.
- CO and O₂ are the only surface fluxes.
- Quiescent atmosphere.
- HO₂ and H₂O₂ are unimportant at the temperatures studied.
- Convective and Conductive gas phase heat transfer only.

TABLE 2. REACTIONS CONSIDERED

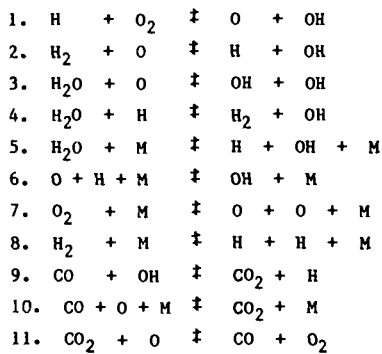


TABLE 3. SOLUTION PROCEDURE

SOLVE FOR A "FIRST CUT" VERSION, $x_{i,1}(y)$

$$B_i \frac{dx_i}{dy} + (\rho_i/\rho)_\infty = F_i \quad 1)$$

with $F_i = 0$ except $F_{CO} = 28/12$, $F_{O2} = -16/12$

NOW WRITE THE SOLUTION AS $x_i = x_{i,1} + x'_i$

where x'_i satisfies the equation

$$D_i \frac{dx'_i}{dy} + (\rho_i/\rho)_\infty = F_i(y) \quad 2)$$

with all $x'_i(y=0) = 0$

Use $x_i(y)$ and the current temperature profile to calculate the terms $S_i(y)$ and $\dot{q}'''(y)$ from the kinetics expressions.

Integrate $S_i(y)$ to get a new $F_i(y)$

SOLVE EQUATION 2) USING THIS $F_i(y)$, 4th Order Runge-Kutta Routine Used

THE SOLUTION IS THE NEW VALUE FOR $x'_i(y)$

SOLVE THE ENERGY EQUATION, GIVEN $\dot{q}'''(y)$ (See next page)

REPEAT UNTIL THE SYSTEM CONVERGES

TABLE 3. SOLUTION PROCEDURE (cont.)

The Energy Equation:

$$\frac{d^2T}{dy^2} + \left[\frac{C \dot{m}'' a}{K_g} \right] \frac{dT}{dy} - \left[\frac{a^2}{K_g y^4} \right] \dot{q}'''(y) = 0 \quad 3)$$

Given a particle temperature, the temperature gradient at the particle surface $\left[\frac{dT}{dy}(y=1) \right]$ is calculated from an energy balance.

$$\frac{dT}{dy}(y=1) = \frac{am''}{K_g} (\text{factor}) - \frac{a\epsilon\sigma T_p}{K_g} + \frac{a\sigma}{K_g} T_w^4$$

where
 factor = ergs released per gram carbon oxidized to CO
 ϵ = emissivity of the char particle (taken as 0.9)
 σ = the Stefan-Boltzman radiation constant

Given these initial conditions, Equation 3 is solved with a 4th order Runge-Kutta routine, marching from $y = 1$ to $y = 0$.

The calculated value $T(y=0)$ is compared with the bulk gas temperature, and the procedure is repeated until convergence is obtained. (Shooting method).

TABLE 4. INPUT PARAMETERS

$\dot{m}''_c = .01, .02, \underline{.03}, .04, .05 \text{ gm/cm}^2/\text{sec}$

$T_g = 1600, 1700, \underline{1800}, 1900, 2000 \text{ K}$

$a = 10, 20, 30, \underline{40}, 50, 60 \text{ microns}$

Species Mass Fractions at infinity:

$O_2 = .0040, \underline{.0820}, 0.124, 0.167, 0.211$

$H_2O = 0.00046, \underline{0.0023}, 0.0046, 0.0116, 0.0236$

$CO_2 = 0.0056$

$CO, O, H, OH, H_2 =$ Calculated from chemical equilibrium.

Ar = The balance.

NOTE: The underlined quantities represent the "base case", measured from experimental results with the Stanford reactor.

TEMPERATURE PROFILES

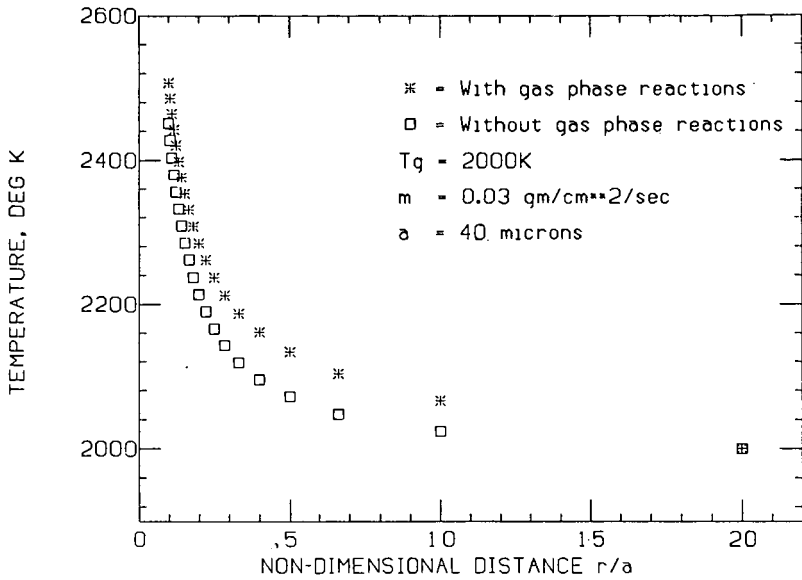


Figure 1. Temperature Profiles.

OXYGEN CONCENTRATION DEPENDENCE

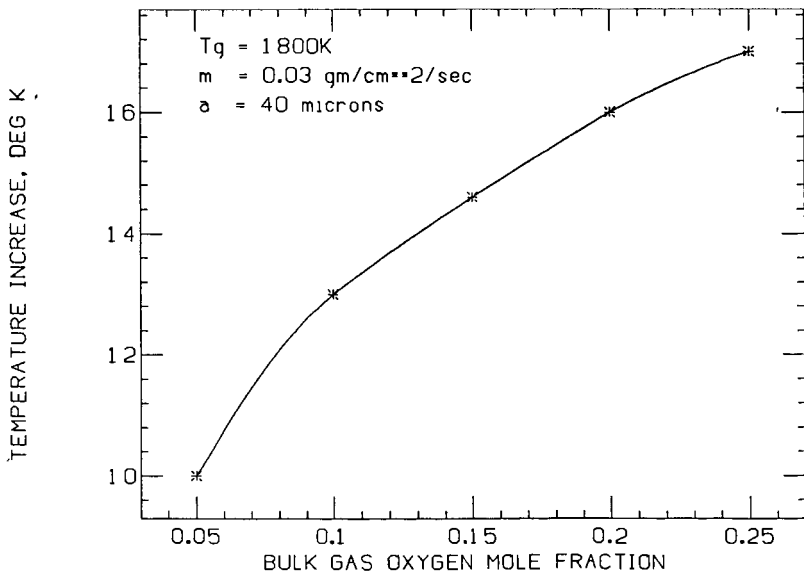


Figure 2. Oxygen Concentration Dependence.

WATER CONCENTRATION DEPENDENCE

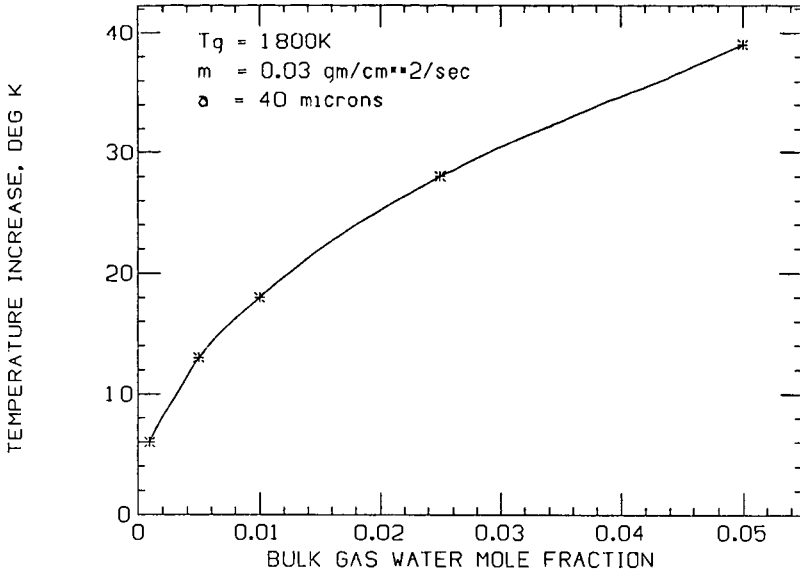


Figure 3. Water Concentration Dependence.

CHAR REACTIVITY DEPENDENCE

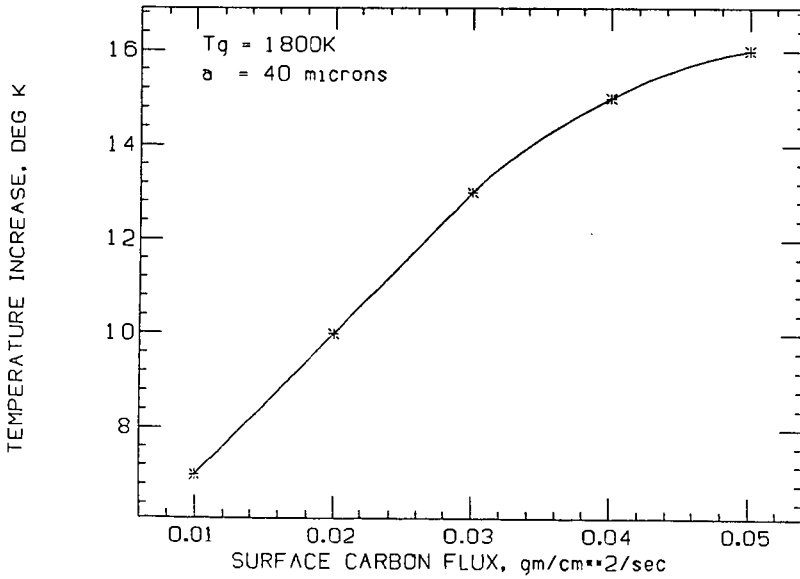


Figure 4. Char Reactivity Dependence.

PARTICLE RADIUS DEPENDENCE

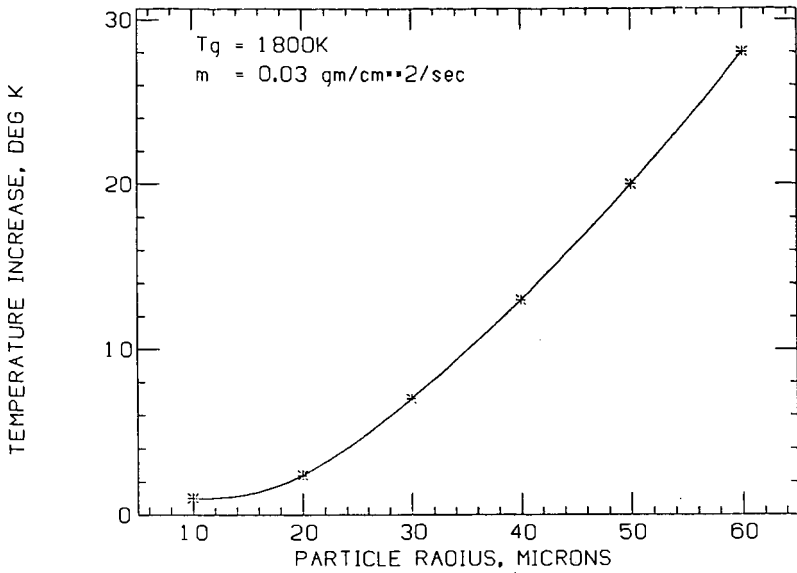


Figure 5. Particle Radius Dependence.

BULK GAS TEMPERATURE DEPENDENCE

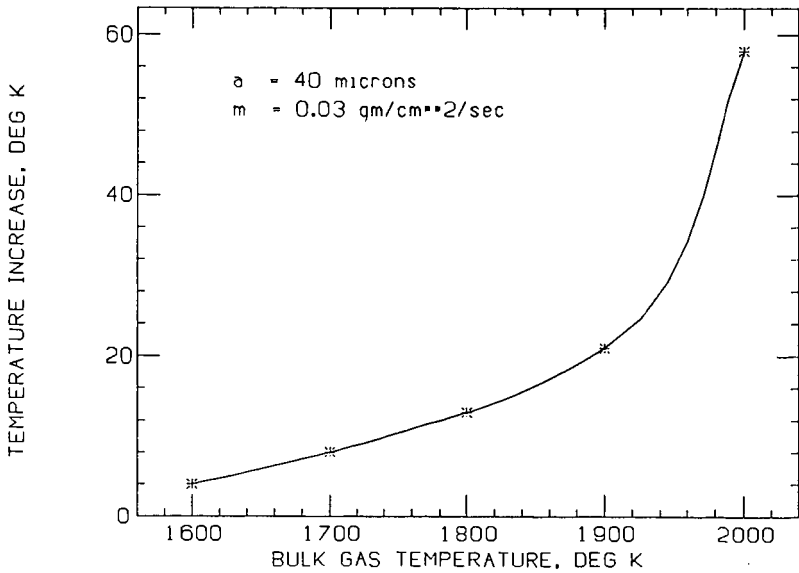


Figure 6. Bulk Gas Temperature Dependence.